Analysis of vacancy and interstitial nucleation kinetics in Si wafers during rapid thermal annealing

2009 J. Phys.: Condens. Matter 21 105402

(http://iopscience.iop.org/0953-8984/21/10/105402)

IOP Publishing Journal of Physics: Condensed Matter

J. Phys.: Condens. Matter **21** (2009) 105402 (11pp) doi:10.1088/0953-8984/21/10/105402

Analysis of vacancy and interstitial nucleation kinetics in Si wafers during rapid thermal annealing

J Kuběna, A Kuběna, O Caha and M Meduňa

Department of Condensed Matter Physics, Masaryk University, Kotlářská 2, 611 37 Brno, Czech Republic

Received 8 September 2008, in final form 7 January 2009
Published 13 February 2009
Online at stacks.iop.org/JPhysCM/21/105402

Abstract

The successful application of the rapid thermal annealing (RTA) process for creation of a magic denude zone in individual Czochralski silicon wafers is based on vacancy controlled oxygen precipitation. The kinetics of the vacancy and self-interstitial processes in Si wafers are studied in this paper. Detailed insight into nucleation processes, out-diffusion and vacancy–interstitial recombination during the RTA leads to a new model of interaction between vacancies and oxygen. The calculation of the distribution function of these defects follows from modified Becker–Döring equations transformed for vacancies and interstitials and extended by diffusion and recombination terms. The new model, which includes the vacancy influence on oxygen nucleation and which follows from this theoretical analysis, corresponds very well to the experimental properties of formation of bulk micro-defects during RTA processes.

1. Introduction

Si wafers pass through a series of thermal operations during production technology of integrated circuits, where oxygen precipitation plays an important role. The dynamics and kinetics of this process has been associated mostly with the interaction of oxygen atoms and vacancies during Si ingot growth in recent years. A series of papers investigate physical models [1–3], which describe growth of bulk micro-defects (BMDs) and their space distribution both along the ingot axis and in the radial direction for various growth rates. These models of BMD evolution during the ingot growth are formulated in a complex way, so that they involve the diffusion effect, crystal growth rate, temperature gradients and mutual interaction between interstitials (I), vacancies (V) and oxygen (O) simultaneously. These results are difficult to apply directly to the processes in individual Si wafers.

It turns out that the process of interaction between vacancies and oxygen in the Si ingot and wafer is not completely clear yet. A search for an appropriate model of these processes continues, for instance in [1, 4–7], which are based on the possibility of formation of various atomic V–O complexes, as suggested by Haley or Prasad [8, 9]. In contrast, papers from Vanhellemont and Frewen [3, 10] are based on intuitive considerations that the essential mechanism is the utilization of vacancies in order to lower the deformation field around oxygen precipitates.

Remarkable attention is paid to the oxidation induced stacking fault ring which is observed on a Czochralski silicon (CZ-Si) wafer after a certain procedure; see, e.g., experimental results in [11]. Such an effect and processes associated with this effect have been analyzed in detail by Frewen [3]. The material parameters of vacancies and interstitials, such as diffusion coefficients and equilibrium concentration, have been more specified on the basis of performed experiments. Rates of recombination and generation as Frenkel pairs per volume were also specified; see [3]. This set of material parameters forms a basis for detailed investigation of individual processes connected with point defects and oxygen inside CZ-Si wafers.

In this paper, we deal with the kinetics of vacancies and interstitial processes during temperature manipulation of Si wafers. We show that a detailed insight into the process kinetics of nucleation, out-diffusion and recombination of vacancies and interstitials during rapid thermal annealing (RTA) allows a calculation of the distribution function of vacancy and interstitial cluster sizes. Mathematical simulations of these processes follow from the modified Becker–Döring (MBD) equations for vacancies and interstitials, which are extended to diffusion and recombination. The solution of the system of differential equations is based on a nodal-point approximation [12]. The detailed calculation of the vacancy

and interstitial cluster distribution function during RTA and subsequent precipitation annealing corresponds well with the experimental results of BMD in CZ-Si wafers.

2. Analysis of processes of vacancies and interstitials in Si wafers

We will restrict ourselves to the RTA process in the theoretical analysis of vacancy and interstitial behavior inside Si wafers. The RTA is based on the heating of the Si wafer to high temperature in a range between 1220 and 1280 °C and then on rapid cooling back to temperatures of 800 °C (cooling velocity in a range from 30 to 100 K s^{-1}). For instance, in order to create the oxygen precipitates with a proper density and gettering efficiency inside the bulk and no precipitates close to the wafer surface, only an annealing at 800 °C for 4 h and further at 1000 °C for 8 h is sufficient after such an RTA procedure. This process is qualitatively described by Falster *et al* [13].

The theoretical study of vacancy and interstitial processes in Si wafers is separated into the following sections:

- kinetics of generation and recombination of Frenkel pairs (vacancy and self-interstitial) in the bulk of the Si wafer without recombination at the sample surface or at boundaries of micro-defects;
- out-diffusion of vacancies and interstitials from the Si wafer to the surface with simultaneous activity of Frenkel pairs;
- investigation of nucleation processes of vacancy and interstitial clusters during simultaneous activity of Frenkel pairs inside the volume of the Si wafer without out-diffusion of vacancies and interstitials to the sample surface;
- study of all three processes simultaneously; generation and recombination of Frenkel pairs, diffusion of vacancies and self-interstitials to the surface and nucleation of vacancy and self-interstitial clusters.

For all simulations in this work, we have used material parameters of vacancies and interstitials published in references [5, 14, 15]. The series of values stated by Frewen [5] forms a complete set of theoretically and experimentally linked parameters, which correspond well to the interpretation of the experiment of spatial distribution of structural defects during the ingot growth with variable growth rates. The values of surface energies at clusters were taken from [14]. All used material parameters are listed in table 1.

2.1. Generation and recombination of Frenkel pairs in bulk Si

The recombination and generation of vacancies and interstitials inside an Si crystal can be realized only as the annihilation and generation of Frenkel pairs. The generation and recombination rate of Frenkel pairs depends on the vacancy and interstitial concentrations by the equation [16]

$$K(t) = -k_{\mathrm{IV}}(T)[c_{\mathrm{I}}(t)c_{\mathrm{V}}(t) - c_{\mathrm{I}}^{\mathrm{eq}}(T)c_{\mathrm{V}}^{\mathrm{eq}}(T)], \qquad (1)$$

where $c_{\mathrm{V}}(t)$ and $c_{\mathrm{I}}(t)$ are the time dependent concentrations of vacancies and self-interstitials, respectively. $c_{\mathrm{V}}^{\mathrm{eq}}(T)$ and $c_{\mathrm{I}}^{\mathrm{eq}}(T)$ denote the corresponding equilibrium concentrations at temperature $T(t)$ and $k_{\mathrm{IV}}(T)$ is the recombination rate coefficient of Frenkel pairs. The temporal evolution of vacancy and interstitial concentrations $c_{\mathrm{V}}(t)$ and $c_{\mathrm{I}}(t)$ is described by the following differential equations:

$$\frac{\mathrm{d}c_{\mathrm{V}}(t)}{\mathrm{d}t} = K(t), \qquad \frac{\mathrm{d}c_{\mathrm{I}}(t)}{\mathrm{d}t} = K(t). \qquad (2)$$

The solution of this system of two differential equations leads to an important conclusion that the difference of vacancy and interstitial concentrations $\Delta = c_{\mathrm{V}}(t) - c_{\mathrm{I}}(t)$ is independent of time and keeps its initial value $\Delta = c_{\mathrm{V}}(0) - c_{\mathrm{I}}(0)$. This is a natural consequence of the fact that the vacancies and interstitials can be generated and recombined only as Frenkel pairs.

The next important attribute of these equations concerns to kinetics of concentrations during the transition from the initial (non-steady) state of vacancy and interstitial concentration to the steady values at temperature T. According to equations (1) and (2), the steady state is reached when the product $c_{\mathrm{I}}(t)c_{\mathrm{V}}(t)$ achieves the value of the product $c_{\mathrm{I}}^{\mathrm{eq}}(T)c_{\mathrm{V}}^{\mathrm{eq}}(T)$. From the condition $K(t) \to 0$ we obtain the following expression for the concentration of vacancies or interstitials at the steady state for a given temperature:

$$c_{\mathrm{V,I}}(t)|_{t\to\infty} = \sqrt{(\Delta/2)^2 + c_{\mathrm{I}}^{\mathrm{eq}}(T)c_{\mathrm{V}}^{\mathrm{eq}}(T)} \pm \Delta/2. \qquad (3)$$

Figure 1(a) shows the temporal evolution of vacancy and interstitial concentrations during annealing at temperatures of 800, 1000 and 1200 °C according to equation (2). It is evident that the initial difference of vacancy and interstitial concentrations Δ is always preserved and the recombination rate strongly depends on annealing temperature. The transition from the initial non-steady values of concentrations to the steady state proceeds within 10^{-1} s at temperature around 1000 °C. A comparison of the concentrations in steady states with equilibrium concentrations at various temperatures is shown in figure 1(b). From the computation it follows that the concentration of vacancies and interstitials is always typically almost in the steady state during the cooling, even at very fast cooling rates, 50–100 K s^{-1}.

For RTA processes an important question can be asked: how the initial vacancy and interstitial concentration difference Δ, larger than the equilibrium one, can be induced inside the crystal. It follows from observations up to now of CZ-Si ingot growth that the oversaturation of vacancies during RTA can be induced for instance by dissolving of nanovoids which remain inside the ingot as an artifact after the vacant growth of the Si crystal. We will pay attention to this effect in the next section of this paper.

2.2. Recombination and diffusion of vacancies and interstitials in an Si wafer

In the following section we will focus on generation and recombination of Frenkel pairs and also on diffusion of

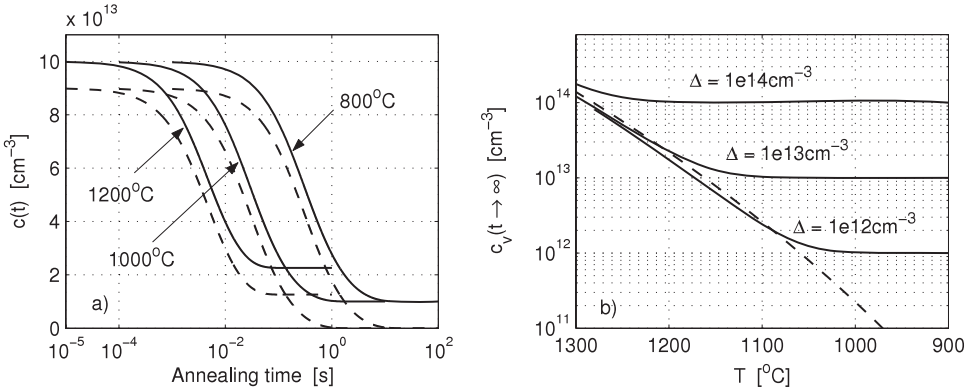

Figure 1. (a) The evolution of concentration of interstitials $c_{\mathrm{I}}(t)$ (dashed line) and vacancies $c_{\mathrm{V}}(t)$ (solid line) during annealing at temperatures 800, 1000 and 1200 °C. The initial difference of c_{I} and c_{V} concentrations $\Delta = 1 \times 10^{13}$ cm^{-3} was chosen. (b) Temperature dependence of the steady state concentration of vacancies for various values of Δ (solid) and equilibrium vacancy concentration (dashed).

Table 1. Material constants used in simulations: monomer volume v, vacancy surface energy σ_{V}, interstitial surface energy σ_{I}, interstitial equilibrium concentration $c_{\mathrm{I}}^{\mathrm{eq}}$, vacancy equilibrium concentration $c_{\mathrm{V}}^{\mathrm{eq}}$, diffusivity of interstitials D_{I}, diffusivity of vacancies D_{V}, and recombination rate coefficient k_{IV}.

$v = 2.0013 \times 10^{-23}$ cm^3	Kulkarni *et al* [14]
$\sigma_{\mathrm{V}} = 5.19 \times 10^{14}$ eV cm^{-2} $= 832$ erg cm^{-2}	Kulkarni *et al* [14]
$\sigma_{\mathrm{I}} = 8.27 \times 10^{14}$eV cm^{-2} $= 1326$ erg cm^{-2}	Kulkarni *et al* [14]
$c_{\mathrm{I}}^{\mathrm{eq}}(T) = 2.98 \times 10^{23} \exp(7.67) \exp(-\frac{4.0\,\mathrm{eV}}{k_{\mathrm{B}}T})$ cm^{-3}	Frewen *et al* [5]
$c_{\mathrm{V}}^{\mathrm{eq}}(T) = 4.97 \times 10^{22} \exp(7.6) \exp(-\frac{3.7\,\mathrm{eV}}{k_{\mathrm{B}}T})$ cm^{-3}	Frewen *et al* [5]
$D_{\mathrm{I}}(T) = 0.237 \exp(-\frac{0.937\,\mathrm{eV}}{k_{\mathrm{B}}T})$ cm^2 s^{-1}	Frewen *et al* [5]
$D_{\mathrm{V}}(T) = 7.87 \times 10^{-4} \exp(-\frac{0.457\,\mathrm{eV}}{k_{\mathrm{B}}T})$ cm^2 s^{-1}	Frewen *et al* [5]
$k_{\mathrm{IV}}(T) = 1.2 \times 10^{-6}(D_{\mathrm{I}} + D_{\mathrm{V}}) \exp(-\frac{(0.58-2.29T-7.38\times10^{-3}T^2)\,\mathrm{eV}}{k_{\mathrm{B}}T})$ cm^3 s^{-1}	Sinno *et al* [15]

vacancies and interstitials towards wafer surfaces. Vacancies and interstitials can be generated and recombined at the surface as single particles and not only as Frenkel pairs. Thus the value of the vacancy and interstitial concentration difference Δ is not preserved during the annealing process. We will assume that the vacancy and interstitial concentrations at the wafer surface correspond to the equilibrium concentrations $c_{\mathrm{V,I}}^{\mathrm{eq}}(T)$. This assumption is correct if the vacancy and interstitial surface recombination and generation is so fast that the equilibrium concentrations are reached almost immediately. Such a condition is satisfied if the annealing is performed in a vacuum and the surface is not covered by any oxide or nitride layers. Akatsuka and others [17] have reported that an annealing in Ar atmosphere also satisfies these assumptions very well.

The out-diffusion process of vacancies and interstitials inside an Si wafer will occur only when the concentration of vacancies or interstitials in volume is larger than the equilibrium concentration. The out-diffusion processes of vacancies and interstitials do not proceed independently of each other, since they are always bound by the volume activity of Frenkel pairs. This relation significantly affects the spatial distribution of vacancy and interstitial concentration inside the Si wafer. We will study the depth profile of vacancy and interstitial concentrations along the x axis perpendicular to the Si wafer surface.

The out-diffusion processes of vacancies and interstitials and the process of volume generation and recombination are described by a system of differential equations according to Frewen *et al* [5].

$$\frac{\partial c_j(t,x)}{\partial t} = K(t,x) + D_j(T)\frac{\partial^2 c_j(t,x)}{\partial t^2}, \qquad (4)$$

where j stands for V or I, x is the position along the axis perpendicular to the wafer surface and $D_{\mathrm{V}}(T)$ and $D_{\mathrm{I}}(T)$ are diffusion coefficients of vacancies and interstitials in silicon, respectively.

We have solved this system of equations numerically for an Si wafer with thickness 0.6 mm and for surface concentrations corresponding to $c_{\mathrm{I}}^{\mathrm{eq}}(T)$ and $c_{\mathrm{V}}^{\mathrm{eq}}(T)$. The initial concentrations of vacancies and interstitials across the wafer were assumed constant with values stated in corresponding figure captions; see figures 2 and 3. Discussion on numerical calculations will be limited to two cases: (i) Si wafer after the vacant growth of crystal $c_{\mathrm{V}}(x,0) > c_{\mathrm{I}}(x,0)$ and (ii) Si wafer after the interstitial growth of crystal $c_{\mathrm{V}}(x,0) < c_{\mathrm{I}}(x,0)$.

2.2.1. Discussion of depth profile calculation for a vacant Si wafer. The simulation results of the vacancy and interstitial concentration depth profile during fast cooling of a vacant Si wafer are plotted in figure 2. The chosen temperature dependence on time is plotted in figure 2(d). The recombination process is active mainly within the first 5 s at temperature 1280 °C, where the concentration profile tends to preserve the initial value of $\Delta = 10^{14}$ cm^{-3} but is also disturbed by out-diffusion. The out-diffusion causes a

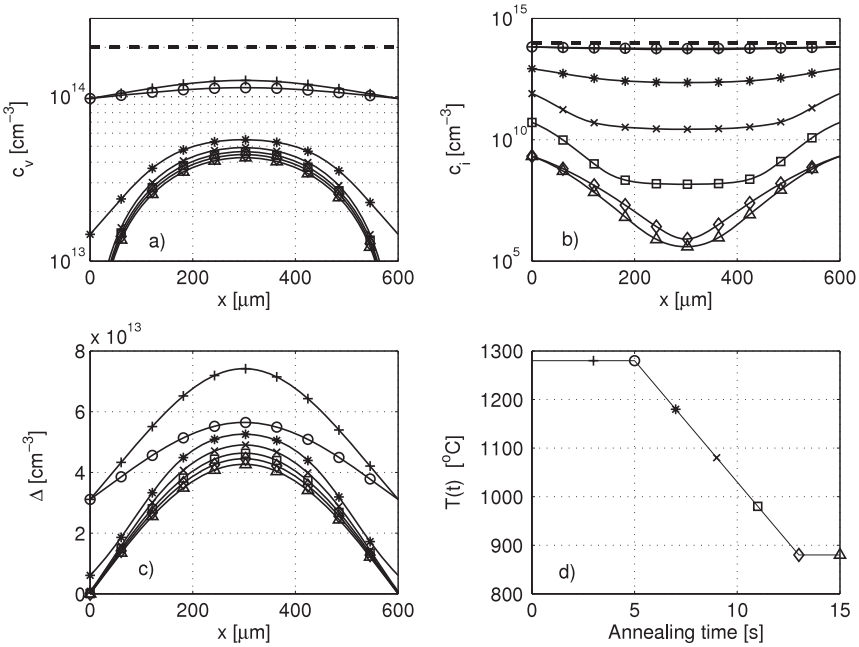

Figure 2. The temporal evolution of interstitial and vacancy concentration depth profile $c_{\mathrm{I}}(t, x)$ (a), $c_{\mathrm{V}}(t, x)$, (b) through a vacant Si wafer with initial values (dash) $c_{\mathrm{I}}(0, x) = 1 \times 10^{14}$ cm^{-3} and $c_{\mathrm{V}}(0, x) = 2 \times 10^{14}$ cm^{-3}. The subplot (c) demonstrates the difference of vacancy and interstitial concentrations $\Delta(t, x)$ at various stages of annealing. The symbols in the plot of the temperature history of the annealing (d) correspond to the symbols in graphs (a), (b) and (c). The cooling velocity is 50 K s^{-1}.

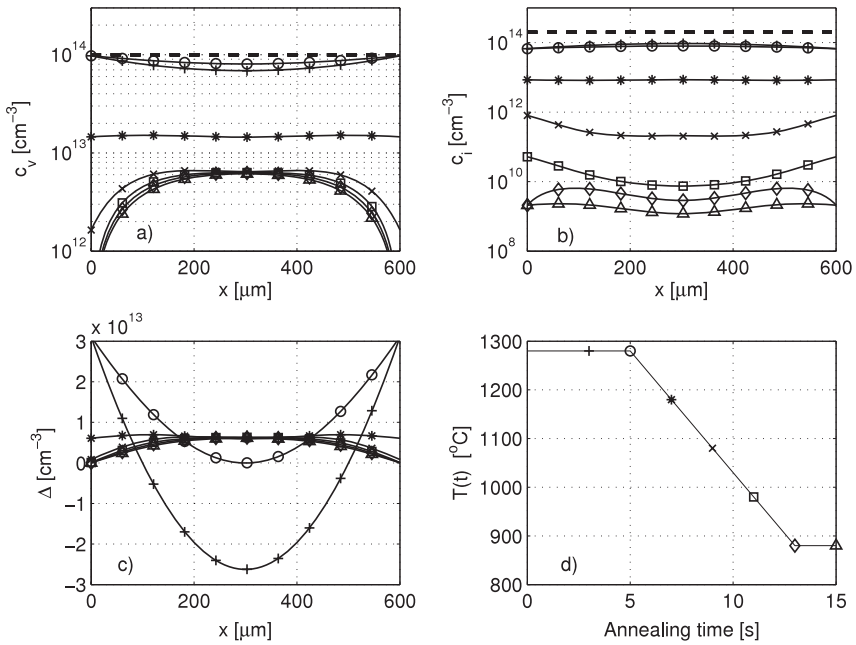

Figure 3. The temporal evolution of interstitial and vacancy concentration depth profile $c_{\mathrm{I}}(t, x)$ (a), $c_{\mathrm{V}}(t, x)$ (b) through an interstitial Si wafer with initial values (dash) $c_{\mathrm{I}}(0, x) = 2 \times 10^{14}$ cm^{-3} and $c_{\mathrm{V}}(0, x) = 1 \times 10^{14}$ cm^{-3}. The subplot (c) demonstrates the difference of vacancy and interstitial concentrations $\Delta(t, x)$ at various stages of annealing. The symbols in the plot of the temperature history of the annealing (d) correspond to the symbols in graphs (a), (b) and (c). The cooling velocity is 50 K s^{-1}.

decrease of vacancy concentration in the direction from the center towards the surfaces of the Si wafer—see figure 2(a).

After the period of the first 5 s, the wafer started to cool down with a rate of 50 K s^{-1}, and this leads to a decrease of the surface concentration. From figure 2(b) we can clearly see the effect of faster out-diffusion of interstitials and also a transition of interstitial out-diffusion into in-diffusion close to the surface. This is the consequence of the tendency of Frenkel pairs to preserve the value of Δ.

2.2.2. Discussion of depth profile calculation in an interstitial Si wafer. The depth profiles of vacancy and interstitial concentrations simulated for the interstitial wafer are plotted

in figure 3. At a temperature of 1280 °C we observe again the tendency to reach the equilibrium vacancy and interstitial concentrations. Similarly as in the vacant wafer, the vacancy concentration reaches a steady value at a temperature of about 1100 °C. The final vacancy concentration $c_V(x)$ at the center of the wafer is about one order lower than for vacant Si wafers within the temperature interval from 1100 down to 900 °C. The shape of the $c_V(x)$ profile depends on the cooling rate and on the initial difference of vacancy and interstitial concentrations. The depth profile of the vacancy and interstitial concentration is also strongly affected by the nucleation of vacancy clusters. All these processes together will be discussed in section 2.4.

2.3. Nucleation and recombination of vacancy and interstitial clusters in bulk Si

In the simulation of the vacancy and interstitial nucleation process we follow the formalism based on the modified Becker–Döring (MBD) equations. This theory describes temporal evolution of clusters whose size is characterized by the number of monomers included. The cluster of a single monomer is understood as an individual vacancy or interstitial. The detailed investigation of properties and solutions of such differential equations by the nodal point method is discussed in our previous paper [12].

The process of nucleation of vacancies and interstitials can be described by two systems of BD equations, one for nucleation of vacancy clusters and the second one for nucleation of self-interstitial clusters. Individual vacancies and interstitials are subjected to generation and recombination of Frenkel pairs, which is represented by a binding term between the vacancy and interstitial system.

The original MBD equations have to be transformed into the shape for clusters of vacancies and interstitials. Indices $j = \mathrm{V}$ or I denote the type of monomer and $i = 1, 2, \ldots$ represents the size of the cluster. The concentration of clusters involving i monomers is denoted as $N_{j,i}(t)$.

The temporal evolution of concentration of clusters size $i \geqslant 2$ is described by the standard BD equations

$$\frac{\mathrm{d}N_{j,i}(t)}{\mathrm{d}t} = k^+_{j,i-1}(t)N_{j,i-1}(t) - [k^+_{j,i}(t) + k^-_{j,i}(t)]N_{j,i}(t) + k^-_{j,i+1}(t)N_{j,i+1}(t), \tag{5}$$

where the growth rate $k^+_{j,i}$ and dissolution rate $k^-_{j,i}$ are given by the expressions

$$k^+_{j,i}(t) = N_{j,1}(t)D_j(T)[4\pi]^{2/3}[3v_j i]^{1/3} \times \exp\left(-\frac{W_{j,i+1} - W_{j,i}}{2k_\mathrm{B}T}\right)$$
$$k^-_{j,i+1}(t) = N_{j,1}(t)D_j(T)[4\pi]^{2/3}[3v_j i]^{1/3} \times \exp\left(\frac{W_{j,i+1} - W_{j,i}}{2k_\mathrm{B}T}\right). \tag{6}$$

The parameter v_j is the monomer volume and $W_{j,i}$ is the free energy of cluster size i

$$W_{j,i} = -\mathrm{i}k_b T \ln\left(\frac{N_{j,1}(t)}{c^{\mathrm{eq}}_j(T)}\right) + [36\pi]^{1/3}[v_j i]^{2/3}\sigma_j, \tag{7}$$

where σ_j is the surface energy of cluster type j.

For clusters of size $i = 1$ we have the equation

$$\frac{\mathrm{d}N_{j,1}(t)}{\mathrm{d}t} = K(t) + Q_j(t) \tag{8}$$

where the terms on the right side of the equation are

$$K(t) = -k_{\mathrm{IV}}(T)[N_{\mathrm{I},1}(t)N_{\mathrm{V},1}(t) - c^{\mathrm{eq}}_{\mathrm{I}}(T)c^{\mathrm{eq}}_{\mathrm{V}}(T)]$$
$$Q_j(t) = -k^+_{j,1}(t)N_{j,1}(t) + k^-_{j,2}(t)N_{j,2}(t) - \sum_{i=2}^{\infty}[k^+_{j,i}(t) - k^-_{j,i}(t)]N_{j,i}(t). \tag{9}$$

The term $K(t)$ represents generation and recombination of Frenkel pairs and the term $Q_j(t)$ is the change of monomer concentration due to growth or dissolution of the corresponding clusters.

Equations (5) and (8) constitute the whole system of differential equations describing simultaneously the nucleation of vacancy and interstitial clusters while preserving the properties following from the activity of Frenkel pairs. These equations can be solved by the nodal point method, as described in [12], using initial conditions $N_{\mathrm{I},1}(0) = c_{\mathrm{I}0}$, $N_{\mathrm{V},1}(0) = c_{\mathrm{V}0}$ and $N_{\mathrm{I},i}(0) = N_{\mathrm{V},i}(0) = 0$ for $i \geqslant 2$.

As well as the distribution function of vacancies $N_\mathrm{V}(t)$ and interstitials $N_\mathrm{I}(t)$ we will also pay attention to the following variables.

- Temporal dependence of *concentration of free vacancies* $c_\mathrm{V}(t) = N_{\mathrm{V},1}(t)$ and *interstitials* $c_\mathrm{I}(t) = N_{\mathrm{I},1}(t)$. Free vacancies and interstitials are characterized by a property that they serve as building units for clusters and they participate in out-diffusion, recombination and generation in real Si wafers.
- *Concentration of vacancy and interstitial clusters*, which is given by the following equation:

$$\chi_j(t) = \sum_{i=n^*}^{\infty} N_{j,i}(t). \tag{10}$$

where n^* denotes the critical cluster size, which satisfies the equation $W_{j,n^*} = W_{j,n^*+1}$. For practical reasons we have used a constant value of $n^* = 10$ in equation (10), which gives results consistent with the correct value of n^*.

2.3.1. Discussion on numerical calculations of nucleation of vacancy and interstitial clusters during RTA.

In the simulation of nucleation properties of vacancy and interstitial clusters we will concentrate in part on the process of dissolution of vacancy clusters (nanovoids) inside Si wafers (the presence of nanovoids is expected in vacant Si crystals), and in part on the nucleation of vacancy and interstitial clusters during the cooling process with various cooling rates.

The nucleation process was simulated using an Si crystal with initial free vacancy concentration 2×10^{14} cm^{-3} and initial free interstitial concentration 1×10^{14} cm^{-3} with no additional clusters of vacancies and interstitials. The results of the simulation of vacancy nucleation during RTA are shown in figure 4 using the temperature history profile from figure 4(d). The temperature profile consists of several annealing phases; we will discuss each of them in the following.

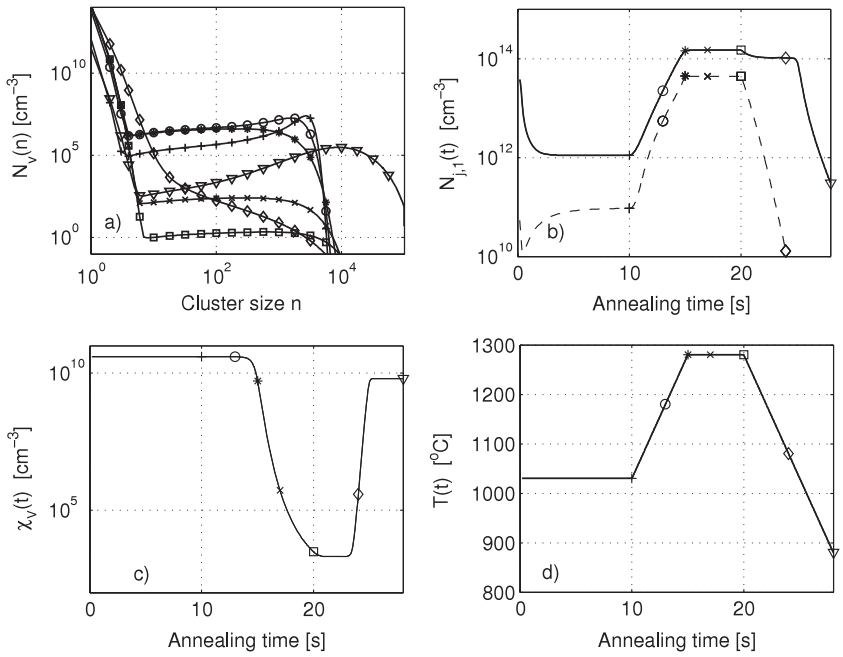

Figure 4. The evolution of vacancy distribution function $N_{\mathrm{V},i}(t)$ (a) during RTA in a vacant Si wafer with initial values $c_{\mathrm{I}}(0) = 1 \times 10^{14}$ cm^{-3} and $c_{\mathrm{V}}(0) = 2 \times 10^{14}$ cm^{-3}. The subplots (b) and (c) show the temporal evolution of the free vacancy (solid line) and interstitial (dashed line) concentrations $N_{j,1}(t, n)$, $j = \mathrm{I}, \mathrm{V}$ and the concentration of vacant clusters $\chi_{\mathrm{V}}(t)$ at various annealing times. The symbols in the plot of the temperature history of the annealing (d) correspond to the symbols in graphs (a), (b) and (c). The cooling velocity was 50 K s^{-1}.

The first annealing phase was chosen to nucleate a number of vacant clusters. The free vacancy and interstitial concentration reach steady state after two seconds and vacancy nucleation proceeded simultaneously (see figures 4(b) and (c)). The concentration difference Δ is not preserved in this case since some of the vacancies were stored in the vacancy clusters (nanovoids). The steady state is characterized by the distribution function in figure 4(a) denoted as (+). The temporal dependence of vacancy cluster concentration $\chi_{\mathrm{V}}(t)$ is shown in figure 4(c).

The interstitial nucleation was not observed during the process. The simulation has shown that only clusters involving two to four interstitial monomers have been formed and their concentration was only of the order of 10^2 cm^{-3}. This result is mainly a consequence of the large surface energy of interstitial clusters.

The dissolution of the vacancy clusters is observed already during heating up to the temperature 1280 °C, and almost all nanovoids dissolve during the period at 1280 °C. This process is clearly shown in figures 4(b) and (c), where free vacancy concentration almost reached the initial value of 2×10^{14} cm^{-3} after its initial decrease at temperature 1030 °C.

The formation of nanovoids is controlled mainly by the oversaturation of free vacancies, and the dissolution of nanovoids proceeds since their size is smaller than the critical size. The changes of the distribution function of vacancies in individual stages of nucleation and dissolution process are evident from the figure 4(a).

Now let us consider the last phase of the RTA process shown in figure 4, when the cooling goes on with a cooling rate of 50 K s^{-1} from temperatures 1280 down to 880 °C. It is important to notice the distribution of the vacancy clusters in figure 4(a), which corresponds to the temperatures from 1280 to 880 °C. These curves clearly demonstrate that the vacancy nucleation continues even at such high cooling rates. From figure 4(c) we can observe that the nanovoid concentration $\chi_{\mathrm{V}}(t)$ at the end of the cooling is of the order of 1×10^{10} cm^{-3}.

In our opinion the quickness with which the nanovoids in the crystal (involving thousands and tens of thousands of monomers) are formed is a fundamental result following from this simulation. The vacancies have an ability to form sufficiently large clusters, in contrast to the interstitials, during the Si wafer cooling with a rate of 50 K s^{-1}. We have found that similar results are also observed for the cooling rate of 100 K s^{-1}. The graph in figure 4(c) shows that temperature close to a value of 1030 °C is essential for the nucleation process.

It follows from the simulations that the temperature level and the period at the high temperature of 1280 °C (see figure 4) is very important. The nanovoids which were formed during crystal growth are diluted into the atomic state during this high temperature annealing phase of the Si wafer. Unfortunately, this temperature level and the length of the period depend on the temperature history of the Si wafer originating from a certain position in the Si ingot. If some old vacancy clusters are not dissolved, the new ones will nucleate and the old ones will still grow. Two groups of nanovoids of two different sizes will then be present in the Si wafer.

2.4. Nucleation and recombination of vacancies and interstitials with out-diffusion in Si wafers

The simulation of all considered processes is based on the system of MBD equations (5) and (8). We have assumed

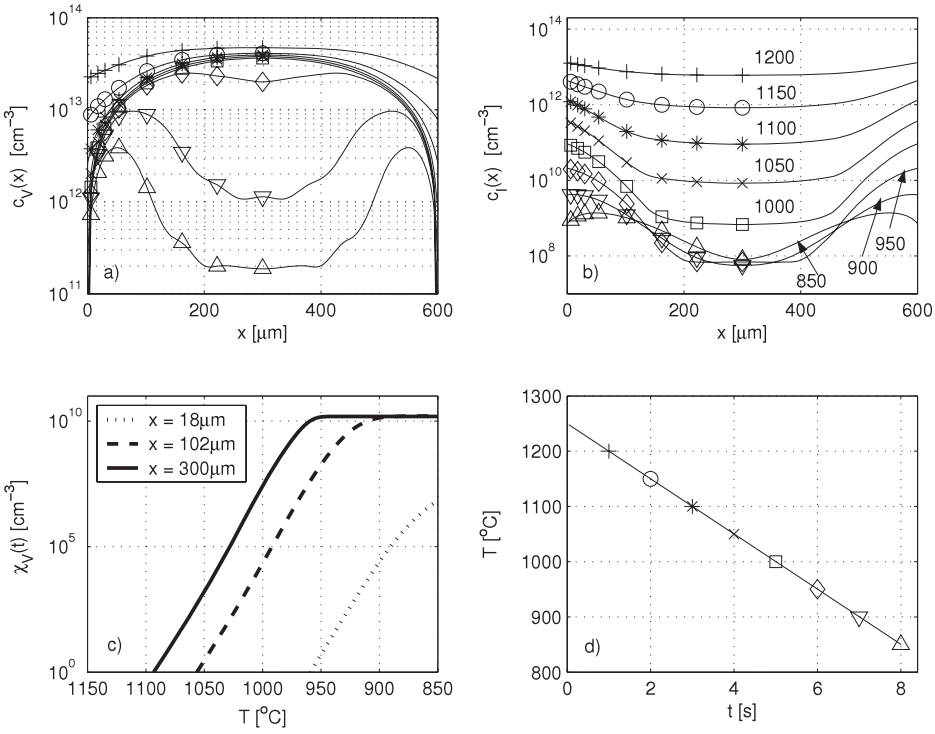

Figure 5. Temporal evolution of vacancy and interstitial concentration depth profile $c_V(t, x)$ (a) and $c_I(t, x)$ (b) during cooling from temperature 1250 to 800 °C with cooling velocity 50 K s^{-1}. The symbols correspond to the symbols in the plot of the temperature temporal dependence (d). (c) The temporal evolution of the vacancy cluster concentration $\chi_V(t, x)$ at three positions in the wafer: close to the surface (18 μm), at the maximum vacancy concentration (102 μm), and in the wafer center (300 μm).

that vacancy and interstitial clusters do not diffuse except the clusters of size 1 (free vacancies and interstitials). This assumption is not valid in the real system and small clusters can diffuse. However, the concentration of small clusters is at least one order of magnitude lower (see figure 4(a)) than the concentration of free monomers. Moreover, the small clusters are not stable and they are rapidly forming from free monomers and dissolving. Their concentration is in thermodynamic equilibrium with the free monomer concentration. Therefore, the effect of small cluster diffusion is minor with respect to the diffusion of free monomers.

The system (5) has to be solved at every position inside the wafer

$$\frac{\partial N_{j,i}(t,x)}{\partial t} = k^+_{j,i-1}N_{j,i-1}(t,x) - [k^+_{j,i} + k^-_{j,i}]N_{j,i}(t,x) + k^-_{j,i+1}N_{j,i+1}(t,x). \quad (11)$$

The first equation of the BD system has to be modified to include free vacancy and interstitial diffusion

$$\frac{\partial N_{j,1}(t,x)}{\partial t} = K(t,x) + Q_j(t,x) + D_j(T)\frac{\partial^2 N_{j,1}(t,x)}{\partial x^2} \quad (12)$$

where the terms K and Q_j are defined by the expressions (9).

2.4.1. Discussion of nucleation and diffusion simulation of RTA. In the following we will study kinetics of all individual processes which involve vacancies and interstitials during cooling from 1250 to 800 °C with a rate of 50 K s^{-1}. This simulation does not include the stages of heating up and delay at high temperature, whose purpose was to dissolve almost all clusters. Our previous simulations showed that dissolution of almost all clusters at a temperature of 1250 °C occurs over several seconds (see figure 4(c)).

The initial state of this simulation was chosen as an equilibrium vacancy and interstitial concentration at temperature 1300 °C with $c_V(0, x) = 1.39 \times 10^{14}$ cm^{-3} and $c_I(0, x) = 0.97 \times 10^{14}$ cm^{-3}. The results are shown in figures 5 and 6. The graphs in figures 5(a) and (b) demonstrate that the initial free vacancy and interstitial concentration has rapidly decreased due to out-diffusion and Frenkel pair recombination already during the first second. The free interstitial concentration in the central part of the wafer decreased even below its equilibrium value for temperature 1200 °C.

Free interstitial concentration decreases even more during next three seconds going to the temperature 1050 °C. Free vacancy concentration decreases much less during this stage in the central part of the wafer and is changed by the out-diffusion only near the surface. During this cooling phase almost no nucleation of vacant clusters has occurred and the results correspond to those described in sections 2.1 and 2.2.

The temperature phase between 1050 and 950 °C is essential for the nucleation of vacant clusters. The rapid growth of vacant clusters can be seen in figure 5(c); the concentration of nanovoids in the wafer center reaches the value of $\chi_V = 1.3 \times 10^{10}$ cm^{-3} at the temperature of 950 °C.

Nucleation of nanovoids is documented by the distribution functions N_V plotted in figures 6(a)–(c) in several positions

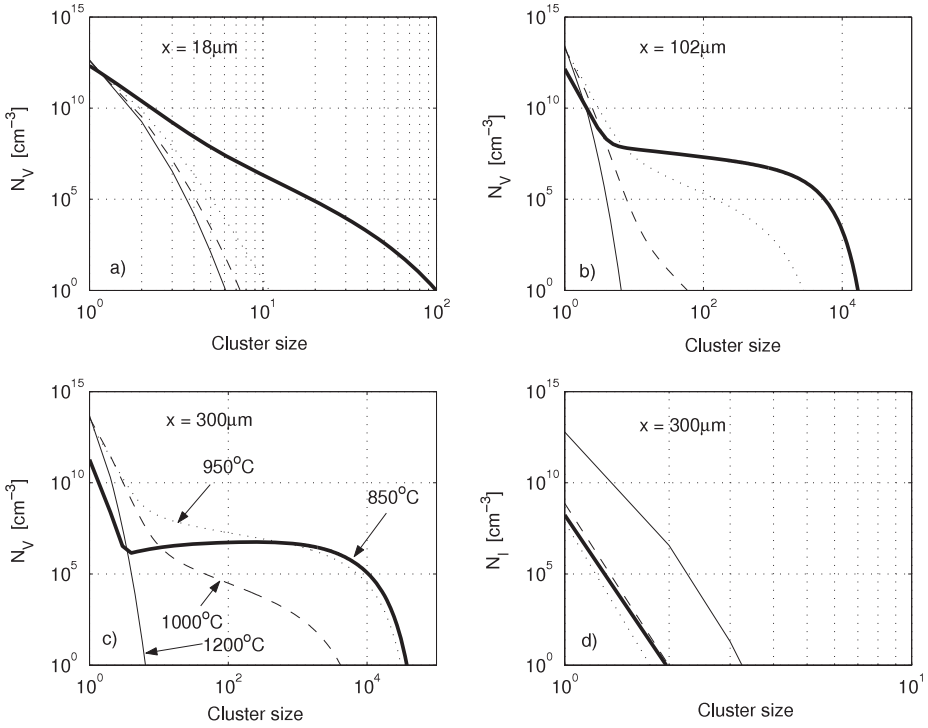

Figure 6. The evolution of vacancy and interstitial cluster distribution function $N_{j,i}(t, x)$ during cooling with velocity 50 K s^{-1}. The subplots show the vacancy cluster distribution $N_{\mathrm{V},i}(t, x)$ in three positions inside the silicon wafer: (a) $x = 18$ μm, (b) $x = 102$ μm, and (c) $x = 300$ μm. Subplot (d) shows the interstitial cluster distribution $N_{\mathrm{I},i}(t, x)$ in the center of the wafer. Various line types correspond to the temperature as shown in subplot (c). The temperature process and starting conditions are the same as in figure 5.

inside the wafer. The nucleation process of vacancy clusters is determined by the free vacancy concentration and therefore the nucleation starts in the wafer center. The effect of vacancy nucleation is a decrease of free vacancy concentration mainly in the wafer center. The natural consequence is low free vacancy concentration in the center and maximum vacancy concentration at a certain depth under the surface depending on the initial conditions and cooling rate. This depth is around 100 μm below the surface in our simulation. The size of vacancy clusters in the wafer reaches values in the interval from 2×10^3 to 1×10^4 vacancies; the corresponding radius of sphere clusters varies in the range from 2.5 to 3.5 nm.

As discussed in section 2.3.1, the nucleation of interstitial clusters is negligible; see also figure 6(d). The simulation shows that surface processes plays an important role in the nucleation in the whole wafer volume. Simulations in this work assume an equilibrium state on the surface characterized only by the temperature. The atmosphere during the annealing and oxide or nitride surface layers can strongly affect the processes inside the wafer. It is evident that the analysis of the wafer surface processes cannot be separated from the volume processes.

3. Sensitivity of the process on the material parameters

In the previous paragraphs we dealt with the analysis of vacancies and self-interstitial processes in the silicon wafer during the RTA process, which leads to the formation of a high density of vacancy clusters. In this paragraph we will study the sensitivity of the RTA process to the particular values of material parameters shown in table 1. The nucleation process can be described by various parameters; we will focus on the total concentration of the vacancy clusters χ_{V}, because in our opinion this values is the most concise parameter. The previous simulations (see e.g. figure 5(c)) showed that the process in the temperature range between 1100 and 1000 °C and cooling rate about 50 K s^{-1} is the most important for vacancy cluster nucleation. For simplicity we will study the vacancy cluster concentration only in the center of the silicon wafer, i.e. at position $x = 300$ μm.

The sensitivity of the vacancy cluster concentration to the various material parameters is shown in figures 7 and 8. As a reference (plotted as a solid line in all panels of both figures) we have used the dependence of the vacancy cluster on the temperature with cooling rate 50 K s^{-1} and initial interstitial and vacancy concentration corresponding to equilibrium values for 1300 °C, and the other parameters have the values presented in table 1. The influence of various material parameters will be compared to this reference dependence.

3.1. Cluster surface energy

The effect of the vacancy cluster surface energy σ_{V} is shown in figure 7(a). The increase of the surface energy σ_{V} decreases the vacancy nucleation rate, which also follows from the nucleation equations (5)–(7). The final value of χ_{V} is lower and the nucleation starts at lower temperature. The decrease

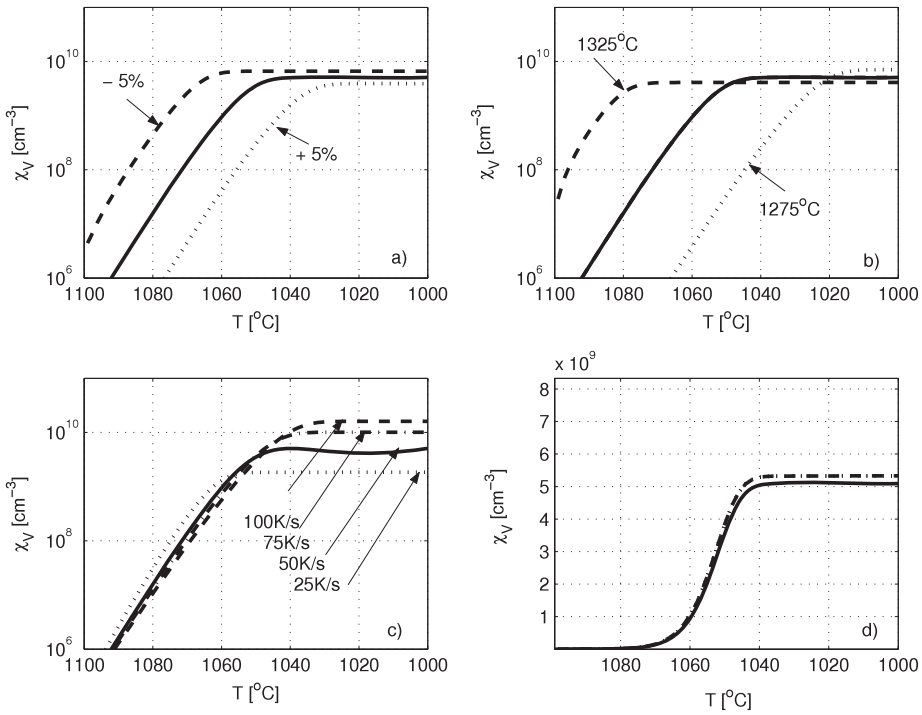

Figure 7. All panels show the dependence of the vacancy cluster concentration on the temperature in the wafer center ($x = 300\,\mu$m) during the rapid cooling process. The solid line in all panels shows the cluster concentration with cooling rate 50 K s^{-1}, initial vacancy and interstitial concentrations corresponding to equilibrium values for 1300 °C and other parameters from table 1. Panel (a) shows the influence of the vacancy surface energy being σ_V higher and lower by $\pm 5\%$; in panel (b) we show the influence of the initial vacancy and interstitial concentration corresponding to the temperatures stated in the figure. Panel (c) shows the process for various cooling rates and the dashed line in panel (d) shows the dependence for the Frenkel pair annihilation parameter k_{IV} being ten times lower.

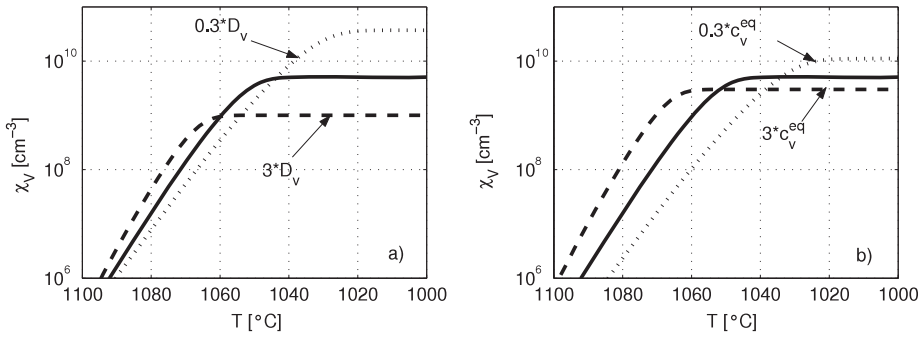

Figure 8. All panels show the dependence of the vacancy cluster concentration on the temperature in the wafer center ($x = 300\,\mu$m) during the rapid cooling process. The solid line shows the cluster concentration for the same parameters as in figure 7. Panel (a) shows the influence of the vacancy diffusion; the dashed and dotted lines show the dependence for the diffusion coefficient multiplied by a factor of 3.0 and 0.3, respectively. The dashed and dotted lines in panel (b) are the dependences for vacancy equilibrium concentration multiplied by a factor of 3.0 and 0.3, respectively.

of the surface energy σ_V leads to an opposite effect. In our simulation we have assumed that the clusters can be well approximated by a spherical shape. This assumption is used in the simulation of ingot growth [2, 4], and atomistic models of vacancy nucleation also suggest that this approximation is valid [3].

Similar changes of surface energy of the interstitial clusters σ_I have negligible effect on the vacancy nucleation since no significant interstitial nucleation was observed in our simulation.

3.2. Initial interstitial and vacancy concentration

The initial value of interstitial and vacancy concentration has a strong effect on the vacancy nucleation—see figure 7(b). The initial concentrations determine the oversaturation of the free vacancies, i.e. the ratio c_V/c_V^{eq}, and its value affects the nucleation in the similar way as the surface energy value σ_V. The initial concentrations depend on the conditions during silicon ingot growth. The vacancies are present in the grown (and cooled) ingot not only as free vacancies but also in

the form of clusters (voids). During the initial stage of the RTA process the voids dissolve (see figure 4) and the initial concentration is restored.

3.3. Cooling rate

The RTA process has two basic phases: short annealing at high temperature of about 1250 °C and subsequent fast cooling. Figure 7(c) shows that with increasing cooling rate the vacancy cluster concentration χ_V increases. With the higher cooling rate the vacancy out-diffusion of vacancies is less pronounced and higher vacancy oversaturation appears in the wafer.

3.4. Frenkel pair recombination rate

Figure 7(d) shows that decrease of Frenkel pair annihilation rate k_{IV} has negligible effect on the vacancy nucleation, even if the value is decreased by a factor of 10. This could be explained by the fact that recombination of vacancies and interstitials occurs almost immediately (see figure 1) and the particular value of this parameter does not play any role in the studied process.

3.5. Diffusivity and equilibrium concentration

The diffusion coefficient is a very important parameter for the nucleation. The values in literature can vary even in the order of magnitude. Each of the four parameter includes two constants: a prefactor and an activation energy describing its temperature dependence by the Arrhenius law. For simple study of vacant clusters in an relatively small temperature range between 1100 and 1000 °C we have just multiplied the diffusion coefficient and equilibrium concentrations by a factor of 3 and 0.3.

In figure 8 one can see that both vacancy diffusion coefficient D_V and equilibrium concentration c_V^{eq} strongly affect the nanovoid concentration. On the other hand, the effect of interstitial diffusion coefficient D_I and equilibrium concentration c_I^{eq} is minor. Similarly, the effect of these parameters on the interstitial nucleation is insignificant, since interstitial nucleation can be neglected. Therefore we do not present analysis of these parameters.

4. Oxygen interaction with nanovoids

The simulation of the RTA process has shown that the nanovoids with a concentration around 1×10^{10} cm^{-3} are formed in the Si wafer and they are situated in the background of the crystal which involves about 10^{18} cm^{-3} oxygen atoms. These nanovoids are well suited nuclei for oxygen precipitation, which can be induced without the initial nucleation lag [18]. The oxygen nucleation inside the nanovoids is energetically preferable to the standard nucleation inside the volume of the crystal lattice since a lower surface energy for oxygen cluster formation can be expected during this process than the surface energy for nucleation in the Si volume.

This formation model of oxygen nuclei of future precipitates already supports several experimental facts published in the context of RTA studies.

- The density of oxygen precipitates is almost independent of the concentration of interstitial oxygen; see [13]. According to our model, the density is determined mainly by the concentration of nanovoids.
- The depth of the magic denude zone region is larger than the region corresponding to oxygen out-diffusion and it is determined by the depth concentration of nanovoids [13].
- A several hour oxygen nucleation annealing at temperature around 650 °C is successfully omitted after application of RTA.
- In order to continue the precipitation at a temperature of 800 °C, the critical size of oxygen clusters inside voids is typically only 30 oxygen monomers for $T = 800$ °C; the size of vacancy clusters in the wafer reaches 2×10^3 to 1×10^4 vacancies. The concentration of oxygen which has to be stored in the voids is of the order of 1×10^{12} cm^{-3}.

5. Conclusion

In this paper we have performed an analysis of vacancy and interstitial nucleation kinetics in Si wafers during the rapid thermal annealing (RTA) process. The analysis is based on the calculation of distribution functions of vacancies and interstitials in various temporal stages of a typical RTA process (cooling from temperature 1250 to 850 °C with cooling rate 50 K s^{-1}).

This investigation of partial process kinetics, involving the vacancies and interstitials during RTA, gives a detailed view of the complex process kinetics, where all the processes interact with each other. We have shown that the nanovoid nucleation occurs at temperatures between 1050 and 950 °C and propagates from the wafer center to the surfaces.

The calculations have shown that a significant nucleation of vacancy clusters is present, which correspond to sizes of several thousand vacancies and with concentration of the order of 10^{10} cm^{-3}. The interstitial clusters are not formed in this process since their formation energy is roughly double the surface energy of vacancy clusters.

We have also formulated a hypothesis that the vacant clusters could be a suitable object where the oxygen nucleation can proceed inside the cluster, since one can expect that the surface energy of the oxygen cluster is lower here than during the nucleation in bulk.

The set of material constants for vacancies and interstitials in Si, which have been used for simulations in this work, are also a suitable set for theoretical description of processes in Si wafers. The theoretical predictions are in agreement with the basic experimental observations about processes during RTA.

Acknowledgments

We would like to acknowledge V Holý for discussions on the theory. This work was part of the projects 202/09/1013 of the Czech Science Foundation and MSM0021622410 of the Ministry of Education of the Czech Republic.

References

[1] Voronkov V and Falster R 1998 *J. Cryst. Growth* **194** 76–88
[2] Kulkarni M S 2005 *Indust. Eng. Chem. Res.* **44** 6246–63
[3] Frewen T A, Kapur S S, Haeckl W, von Ammon W and Sinno T 2005 *J. Cryst. Growth* **279** 258
[4] Kulkarni M S 2007 *J. Cryst. Growth* **303** 438
[5] Frewen T A and Sinno T 2006 *Appl. Phys. Lett.* **89** 191903
[6] Zhong L, Ma X, Tian D and Yang D 2006 *Physica* B **376** 169
[7] Kissinger G, Dabrowski J, Sattler A, Müller T, Richter H and von Ammon W 2007 *J. Electrochem. Soc.* **154** H454
[8] Haley B P, Beardmore K M and Grønbech-Jensen N 2006 *Phys. Rev.* B **74** 45217
[9] Prasad M and Sinno T 2003 *Phys. Rev.* B **68** 45206
[10] Vanhellemont J, De Gryse O and Clauws P 2003 *Physica* B **340** 1056
[11] Válek L, Šik J and Lysáček D 2008 *Solid State Phenom.* **131** 167
[12] Kuběna J, Kuběna A, Caha O and Mikulík P 2007 *J. Phys.: Condens. Matter* **19** 496202
[13] Falster R, Voronkov V V and Quast F 2000 *Phys. Status Solidi* b **222** 219
[14] Kulkarni M S, Voronkov V and Falster R 2004 *J. Electrochem. Soc.* **151** G663–78
[15] Sinno T, Brown R A, von Ammon W and Dornberger E 1998 *J. Electrochem. Soc.* **145** 302
[16] Frewen T A, Sinno T, Haeckl W and von Ammon W 2005 *Comput. Chem. Eng.* **29** 713
[17] Akatsuka M, Okui M, Morimoto N and Sueoka K 2001 *Japan. J. Appl. Phys.* **40** 3055
[18] Kato M, Yoshida T, Ikeda Y and Kitagawara Y 1996 *Japan. J. Appl. Phys.* **35** 5597